

Real Time Green's Functions from NCA based Impurity Solver

Tel Aviv University

9/02/2018

Introduction

Strongly correlated materials.

- Idea of description of electrons in solids as independent particles
→ wave-like picture
- Materials in which electrons tend to *localize*
→ particle-like picture
- Strong electronic correlations brings out a variety of phenomena, e.g. metal-to-Mott-insulator transitions

Description of the lattice

Hubbard model.

$$H_{\text{Hubbard}} = - \sum_{\langle i,j \rangle, \sigma} t_{ij} d_{i\sigma}^\dagger d_{j\sigma} + \sum_i U (d_{i\uparrow}^\dagger d_{i\uparrow} - \frac{1}{2})(d_{i\downarrow}^\dagger d_{i\downarrow} - \frac{1}{2})$$

- $t_{ij} \simeq$ overlap between orbitals on neighbouring atomic sites $\sim \text{eV}$
- Coulomb repulsion U , screened value $\sim \text{eV}$

→ competition between energy scales

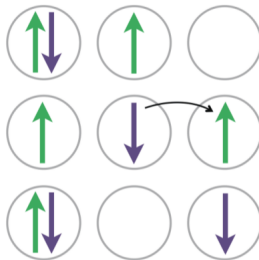


Figure 1: Lattice model

source: H. Aoki, N. Tsuji, M. Eckstein, M. Kollar, T. Oka, and P. Werner, Rev. Mod. Phys. 86, 779 (2014)

Dynamical Mean Field Theory

Idea of mapping.

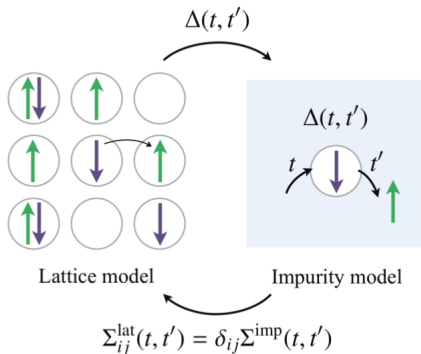


Figure 2: Mapping of the lattice problem onto an Impurity problem

- Approximate lattice problem with many degrees of freedom by *single-site problem*

Dynamical Mean Field Theory

Set of self-consistent equations.

- compute local Greens function $G_{ii}^{\sigma}(t-t') = -i\langle \mathcal{T} d_{i\sigma}(t) d_{i\sigma}^{\dagger}(t') \rangle$ from an effective impurity model with action

$$S = i \int_c dt U n_{\uparrow}(t) n_{\downarrow}(t) - i \sum_{\sigma} \int_c dt dt' d_{\sigma}^{\dagger}(t) \Delta(t-t') d_{\sigma}(t').$$

- use impurity self energy, defined via $G_{ii}^{-1}(\omega) = \omega + \mu - \Delta(\omega) - \Sigma^{imp}(\omega)$, to obtain the lattice Greens function

$$G_{ij}^{-1}(\omega) = \delta_{ij}[\omega + \mu - \Sigma_{ii}(\omega)] - v_{ij}$$

$$\Sigma_{ii}(\omega) \simeq \Sigma^{imp}(\omega); \Sigma_{i \neq j}(\omega) \simeq 0$$

- average over the Brillouin zone to get the on-site component:

$$G_{ii}(\omega) = \frac{1}{L} \sum_{\mathbf{k}} G_{\mathbf{k}}(\omega) = \frac{1}{L} \sum_{\mathbf{k}} \frac{1}{\omega + \mu + \Sigma(\omega) - \epsilon_{\mathbf{k}}}$$

Dynamical Mean Field Theory

Set of self-consistent equations.

$$\mathcal{G}_0 = \omega + \mu - \Delta(\omega)$$

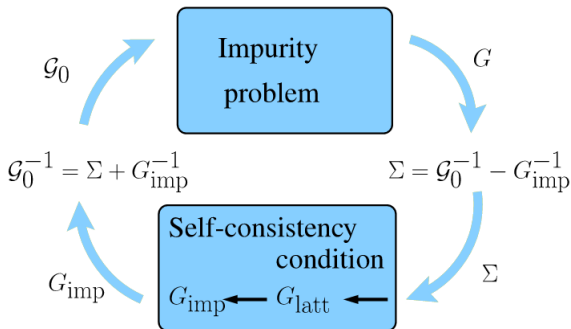


Figure 3: DMFT iterative loop

source: B. Amadon, Journal of Physics: Condensed Matter, Volume 24, Number 7

Real Time Impurity Solver

Pertubative expansion.

Single-orbital Anderson impurity model

$$H_{\text{imp}} = H_{\text{loc}} + H_{\text{bath}} + H_{\text{hyb}}$$

$$H_{\text{loc}} = \sum_{\sigma \in \uparrow, \downarrow} \epsilon_{\sigma} d_{\sigma}^{\dagger} d_{\sigma} + U(n_{\uparrow} - \mu)(n_{\downarrow} - \mu)$$

$$H_{\text{bath}} = \sum_{\sigma, \lambda} \epsilon_{\lambda} b_{\lambda}^{\dagger} b_{\lambda}$$

$$H_{\text{hyb}} = \sum_{\sigma, \lambda} (v_{\sigma\lambda} b_{\lambda}^{\dagger} d_{\sigma} + v_{\sigma\lambda}^{*} d_{\sigma}^{\dagger} b_{\lambda})$$

- Write impurity Hamiltonian as a sum $H_{\text{imp}} = H_0 + H_{\text{int}}$
- Exact time evolution for H_0 , pertubative expansion for H_{int}

Real Time Impurity Solver

Calculation of expectation values.

- Goal is to evaluate objects like $G^<(t,t') = i\langle d^\dagger(t')d(t) \rangle$ and $G^>(t,t') = -i\langle d(t)d^\dagger(t') \rangle$
- Expectation values are given by $\langle O(t) \rangle = \text{Tr}(\rho U^\dagger(t) \hat{O} U(t))$
- Interaction picture propagator $U(t) = \exp^{iH_0 t} \exp^{-iH t}$ and operator $\hat{O}(t) = \exp^{iH_0 t} O \exp^{-iH_0 t}$
- Reduced Hamiltonian $H_0 = H_{\text{imp}} - H_{\text{hyb}}$

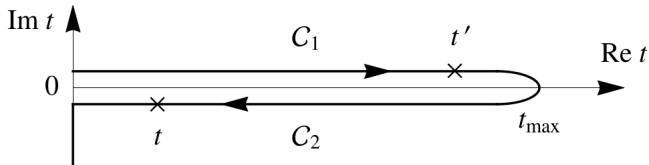


Figure 4: Keldysh Contour

source: H. Aoki, N. Tsuji, M. Eckstein, M. Kollar, T. Oka, and P. Werner, Rev. Mod. Phys. 86, 779 (2014)

Real Time Impurity Solver

Hybridization expansion.

- Expansion of $U(t)$ and $U^\dagger(t)$ in terms of \hat{H}_{hyb} :

$$U(t) = \sum_{n=0}^{\infty} (-i)^n \int_0^t dt_1 \int_0^{t_1} dt_2 \cdots \int_0^{t_{n-1}} dt_n \hat{H}_{\text{hyb}}(t_1) \hat{H}_{\text{hyb}}(t_2) \cdots \hat{H}_{\text{hyb}}(t_n)$$

- Insert expansion for $U(t)$ into propagator between many body states:

$$G_{\alpha\beta}(t) = \langle\langle \alpha | \rho_D \exp^{-iHt} | \beta \rangle\rangle_B = \langle\langle \alpha | \rho_D \exp^{-iH_0 t} U(t) | \beta \rangle\rangle_B$$

- many body states are $|0\rangle, |\uparrow\rangle, |\downarrow\rangle, |\uparrow\downarrow\rangle$
- $\langle\cdots\rangle_B = \text{Tr}\{\rho_B \cdots\}$

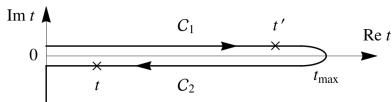


Figure 5: Keldysh Contour

Real Time Impurity Solver

Hybridization expansion.

$$G_{\alpha\alpha}(t) = G_{\alpha\alpha}^{(0)}(t) - \sum_{\gamma\delta} \int_0^t dt_1 \int_0^{t_1} dt_2 G_{\alpha\alpha}^{(0)}(t-t_1) G_{\beta\beta}^{(0)}(t_1-t_2) \Delta_{\alpha\beta}^{\gamma\delta}(t_1-t_2) G_{\alpha\alpha}^0(t_2) - \dots$$

with bare propagators

$$G_{\alpha\alpha}^{(0)}(t) = \langle \langle \alpha | \rho_D \exp^{-iH_0 t} | \alpha \rangle \rangle_B = \exp^{-i\varepsilon_\alpha t}$$

and Hybridization

$$\Delta_{\alpha\beta}(t_1-t_2) = \langle \alpha | d_\sigma | \beta \rangle \langle \beta | d_\sigma^\dagger | \alpha \rangle \Delta^<(t_1-t_2) + \langle \alpha | d_\sigma^\dagger | \beta \rangle \langle \beta | d_\sigma | \alpha \rangle \Delta^>(t_1-t_2)$$

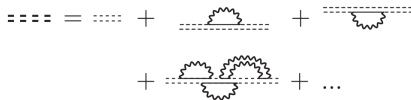


Figure 6: Example of diagrammatic expansion for bold propagators

Real Time Impurity Solver

Hybridization expansion.

Dyson equation

$$G_{\alpha\alpha}(t) = G_{\alpha\alpha}^{(0)}(t) + \int_0^t dt_1 \int_0^{t_1} dt_2 G_{\alpha\alpha}^{(0)}(t-t_1) \Sigma_{\alpha\alpha}(t_1-t_2) G_{\alpha\alpha}(t_2)$$

$$\Sigma_{00} = \text{diagram 1} + \text{diagram 2}$$

$$\Sigma_{11} = \text{diagram 3} + \text{diagram 4}$$

$$\Sigma_{22} = \text{diagram 5} + \text{diagram 6}$$

$$\Sigma_{33} = \text{diagram 7} + \text{diagram 8}$$

Self-consistent solution

- 1 Initialize $G_{\alpha\alpha}(t)$ with $G_{\alpha\alpha}^{(0)}(t)$
- 2 Compute self-energy $\Sigma_{\alpha\alpha}(t)$
- 3 Update $G_{\alpha\alpha}(t)$
- 4 go back to step 2

Figure 7: NCA Self-energy

source: G. Cohen, D. R. Reichman, A. J. M. and E. Gull; Phys. Rev. B89, 112139(2014)

Real Time Impurity Solver

Hybridization expansion.

Vertex functions

$$K_{\alpha\beta}(t, t') = K_{\alpha\beta}^{(0)}(t, t') + \sum_{\gamma\delta} \int_0^t dt_1 \int_0^{t'} dt_2 K_{\alpha\gamma}(t_1, t_2) \triangle_{\gamma\delta}(t_1, t_2) G_{\delta\beta}^\dagger(t - t_1) G_{\delta\beta}(t' - t_2).$$

$$K_{\alpha\beta}^{(0)}(t, t') = G_{\alpha\beta}^\dagger(t) G_{\alpha\beta}(t')$$

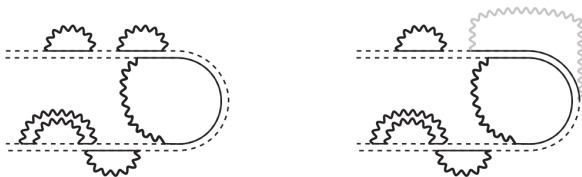


Figure 8: Diagrammatic expansion for Vertex functions

System

Bethe lattice in the initial Néel state.

Self-consistency condition

$$\Delta_{A(B),\sigma}(t,t') = v(t)G_{B(A),\sigma}(t,t')v^*(t')$$

Time-dependent electric field

$$H_{\text{drv}}(t) = \sum_j e a E_0 \sin(\omega t) s_j n_j$$

$$v_{ij}(t) = v_{ij} \exp^{iA(s_i - s_j) \cos(\omega t)}$$

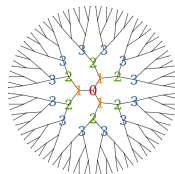


Figure 9: Structure of the Bethe lattice

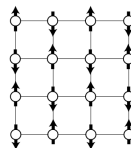


Figure 10: Classical anti-ferromagnetic Néel-state

Open systems

Free-fermion bath

$$H_{\text{tot}} = H_{\text{imp}} + H_{\text{fBath}} + H_{\text{fmix}}$$

$$H_{\text{fBath}} = \sum_{k,\sigma} \epsilon_k f_{k,\sigma}^\dagger f_{k,\sigma}$$

$$H_{\text{fmix}} = \sum_{k,\sigma} (V_k f_{k,\sigma}^\dagger d_\sigma + V_k^* d_\sigma^\dagger f_{k,\sigma})$$

$$G(t, t') = (G_0^{-1}(t, t') - \Sigma_{\text{fBath}}(t, t') - \Sigma(t, t'))^{-1}$$

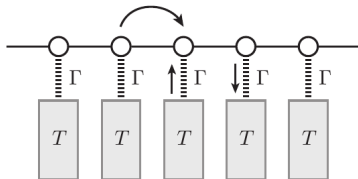


Figure 11: Schematic representation of a free-fermion bath model

Results

How does the ability to dissipate energy change in a non-equilibrium state?

$$I_E(t) = \langle \mathcal{J}_E(t) \rangle \text{ with } \mathcal{J}_E = \dot{H}_{fBath} = i \sum_{k,\sigma} \varepsilon_k (V_k d_\sigma f_{k,\sigma}^\dagger - V_k^* f_{k,\sigma} d_\sigma^\dagger)$$

$$P_{\omega_{probe}}(A_{probe}) = \lim_{A_{probe} \rightarrow 0} \frac{dI_E(A_{probe}(\omega_{probe}))}{dA_{probe}(\omega_{probe})} \simeq \frac{I_E(\Delta A_{probe}(\omega_{probe}))}{\Delta A_{probe}(\omega_{probe})}$$

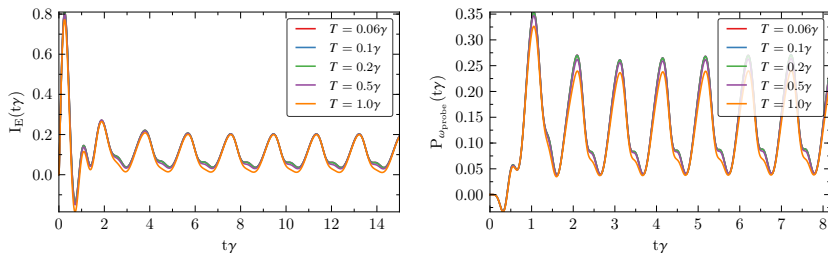


Figure 12: Example of heat current (left) and response (right) at resonant driving for a pump amplitude $A = 1.0$ and a probe field with parameters $\omega_{probe} = 5$ and $A_{probe} = 0.1$.

Results

Response of heat current at resonant driving.

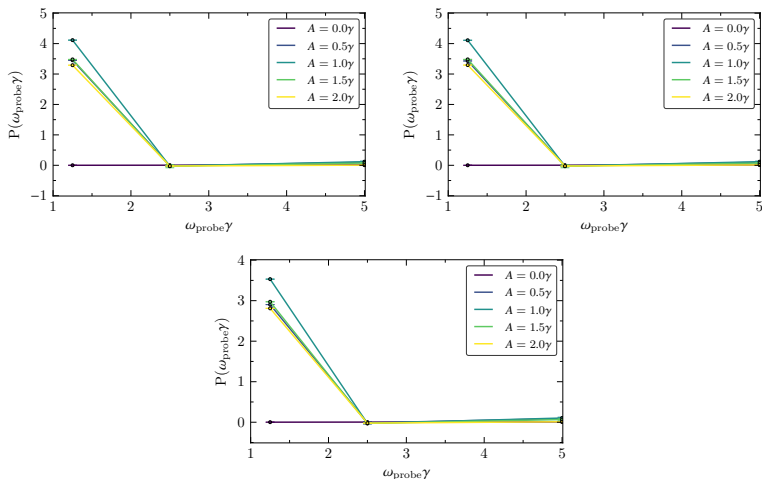


Figure 13: From left to right and top to bottom: $T = 0.06\gamma$, $T = 0.2\gamma$, $T = 1.0\gamma$

Results

Response of heat current at resonant driving.

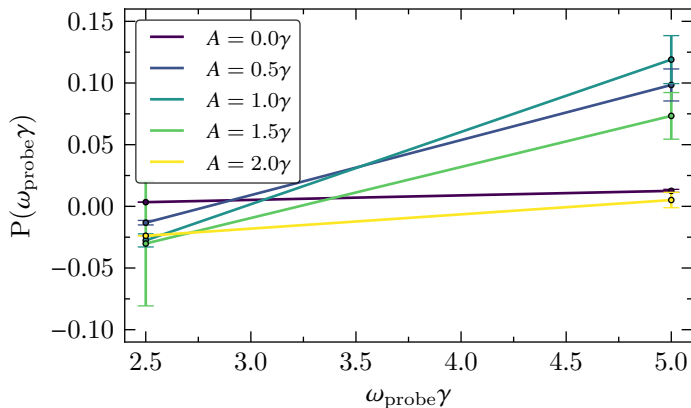


Figure 14: Zoom into $T = 0.06\gamma$

Results

Time evolution of spectral fuctions for various amplitudes at resonant driving.

$$G^r(t, t') = \Theta(t - t')(G^>(t, t') - G^<(t, t'))$$

$$A(\omega) = -\frac{1}{\pi} \text{Im} G^r(\omega)$$

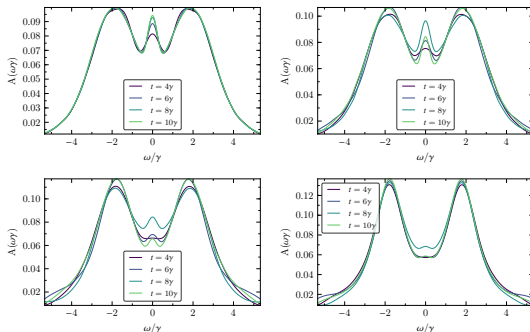


Figure 15: Time evolved spin-averaged spectral functions for $T = 0.06\gamma$. Top left $A_{\text{amp}} = 0.0$, top right $A = 0.5$, bottom left $A = 1.0$ and bottom right $A = 2.0$.

Results

Steady-state spectral fuctions for various amplitudes at resonant driving.

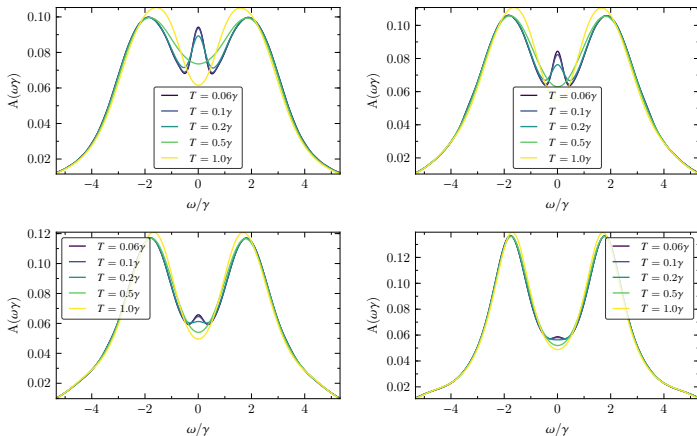


Figure 16: Spectral function averaged over initial spin up and spin down state. Top left $A = 0.0$, top right $A = 0.5$, bottom left $A = 1.0$ and bottom right $A = 2.0$.

Results

Response of heat current at half-resonant driving.

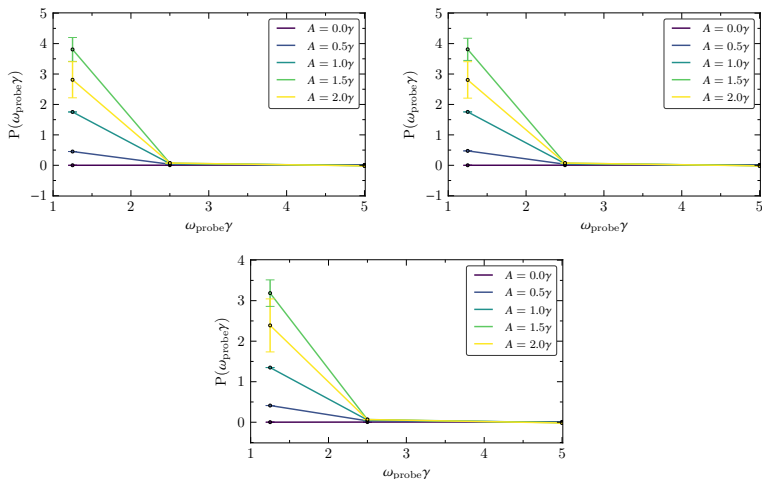


Figure 17: From left to right and top to bottom: $T = 0.06\gamma$, $T = 0.2\gamma$, $T = 1.0\gamma$

Results

Response of heat current at half-resonant driving.

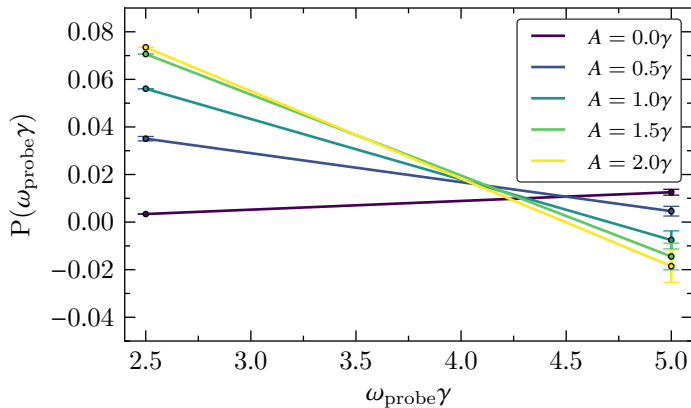


Figure 18: Zoom into $T = 0.06\gamma$

Results

Time evolution of spectral fuctions for various amplitudes at half-resonant driving.

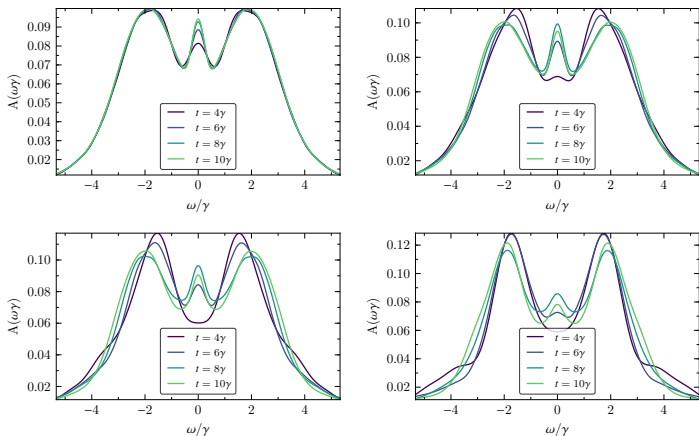


Figure 19: Time evolved spin-averaged spectral functions for $T = 0.06\gamma$. Top left $A_{ump} = 0.0$, top right $A = 0.5$, bottom left $A = 1.0$ and bottom right $A = 2.0$.

Results

Spectral fuctions for various amplitudes at half-resonant driving.

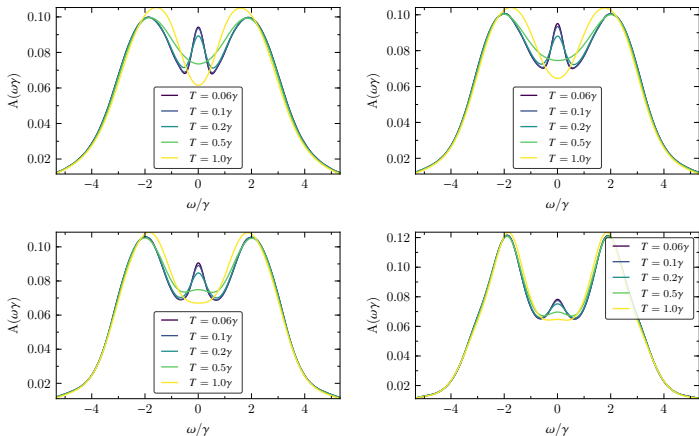


Figure 20: Spectral functions averaged over initial spin up and spin down state. Top left $A = 0.0$, top right $A = 0.5$, bottom left $A = 1.0$ and bottom right $A = 2.0$.

